Assessing the impact of mantle chemistry on surface mobility and the generation of rigid plates in numerical mantle convection models

C.W. Fairservice, J.P. Lowman

Physical & Environmental Sciences
UNIVERSITY OF TORONTO
SCARBOROUGH

Abstract

The theory of plate tectonics describes the surface expression of convection in the Earth's mantle. The mantle is a spherical shell of silicate rocky material enveloping the Earth's metallic core. Obtaining a mobile, plate-like surface from computational mantle convection simulations is a major objective in the study of geodynamics, as is investigating feedback between the chemical composition of the mantle and surface mobility. Seismic tomography data finds that there are features in the Earth's lower mantle well-described as large, low-shearwave-velocity provinces (LLSVPs) that may be chemically distinct from the ambient mantle.

The purpose of this research project is to identify and evaluate the rigidity of plates on the surface of 3D mantle convection simulations and to investigate the evolution of 2D simulations when a compositionally anomalous and intrinsically dense (CAID) material is introduced in the deep mantle.

Mantle convection is modelled using the Digital Alliance of Canada's high-performance computers, where equations for mass, momentum, energy, and composition conservation are solved numerically using the finite volume, parallelized, fluid dynamic modelling code STAGYY, along with an equation of state.

$$\boldsymbol{\nabla} \cdot \mathbf{u} = 0$$

$$\boldsymbol{\nabla} \cdot [\eta(\boldsymbol{\nabla}\mathbf{u}) + (\boldsymbol{\nabla}\mathbf{u})^{\mathrm{T}}] - \boldsymbol{\nabla}\mathrm{P} = -(\mathrm{Ra_T T} + \mathrm{Ra_C C})\hat{\boldsymbol{r}}$$

$$\frac{\partial T}{\partial t} = \nabla^2 \mathrm{T} - \mathbf{u} \cdot \boldsymbol{\nabla}\mathrm{T} + \mathrm{H}$$

$$\frac{\partial \mathrm{C}}{\partial t} = -\mathbf{u} \cdot \boldsymbol{\nabla}\mathrm{C}$$

$$\rho(\mathrm{T}, \mathrm{C}) = \rho_0[1 + \alpha\Delta T(BC - T)]$$

In these equations, $\mathbf{u}$ is velocity, η is dynamic viscosity, P is the nonhydrostatic pressure, T is temperature, t is time, H is the nondimensional internal heating rate, $\mathrm{Ra_C}$ is the compositional Rayleigh number, $\mathrm{Ra_T}$ is a reference Rayleigh number, C is the composition field, B is the buoyancy ratio, and α is the thermal expansivity.

Both 2D and 3D models vary a system property termed the yield stress, σ_{yield}. Implementation of a yield stress in the models allows for the formation of boundaries that separate stiff, cold plates.

Plate boundaries are detected on 3D model surfaces by applying a watershed transform at three separate tolerances to the logarithm of the second invariant of the strain rate tensor field.

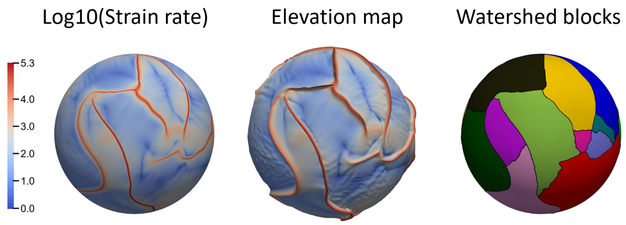

Figure A. Left: the logarithm of the second invariant of the strain rate tensor field at the surface of a model featuring $\sigma_{yield} = 2 \times 10^7 (110\ \mathrm{MPa})$. Centre: the surface field on the left visualized as an elevation map. Right: application of a watershed algorithm at threshold 20%.

To test the validity of detected plates in the models, a uniform sampling of values obtained for the surface velocities are plotted against the expected velocities for a perfectly rigid plate rotating about a corresponding statistically determined axis on the sphere's surface, in accord with Euler's rotation theorem.

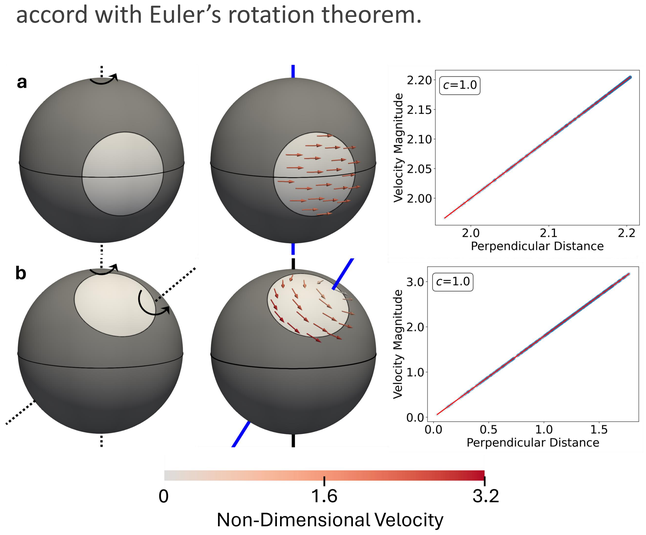

Figure B. Two ideal synthetic plates are shown. The left column illustrates the rotation scenario, the centre column indicates the geographic pole (solid black line), the Euler pole (solid blue axis) and the velocity field of the plate. The right column plots the velocity distribution of the output data relative to its perpendicular distance from the Euler pole.

In 2D models, CAID material viscosity contrast (D) and buoyancy ratio (B) were varied. The viscosity contrast is the ratio of CAID material viscosity to that of the ambient mantle. The buoyancy ratio quantifies the relative importance of thermal buoyancy forces to compositional buoyancy forces.

Conclusions

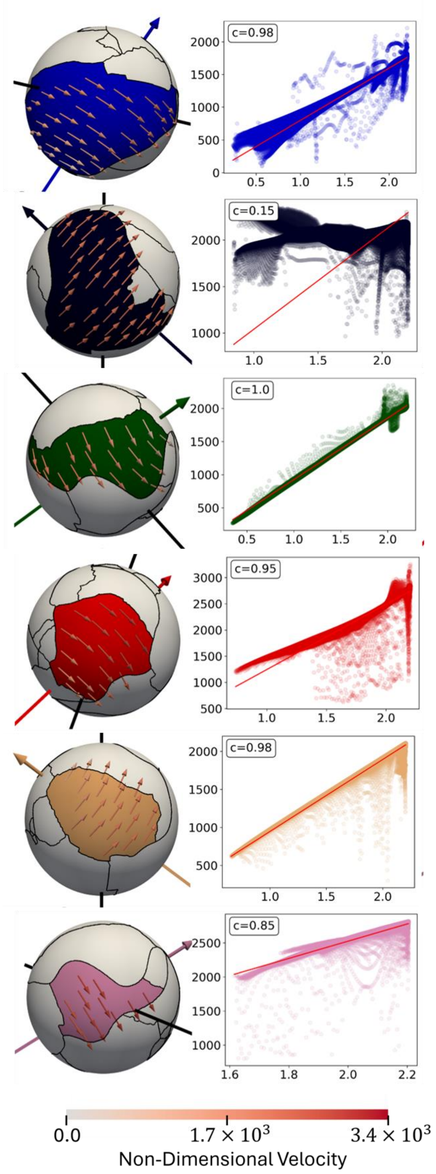

Figure C. The largest six plates with corresponding velocity distribution (threshold 20%) in the calculation featuring $\sigma_{yield} = 2 \times 10^7 (110\ \mathrm{MPa})$. The geographic pole is indicated by a solid black line and the Euler poles are indicated by coloured arrows, where the arrowhead indicates rotation vector direction.

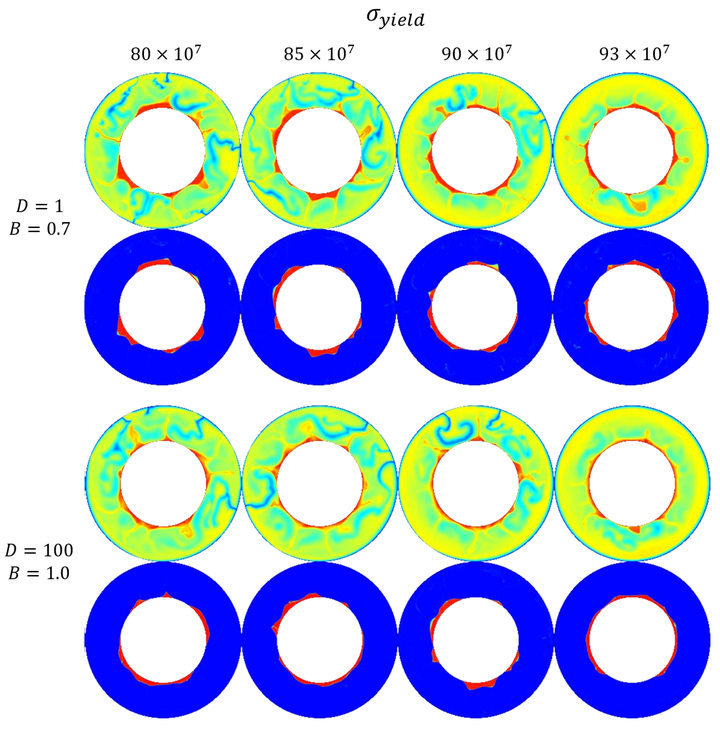

Figure D. Four 2D spherical annulus models are shown with varying non-dimensional yield stress, grouped into two different combinations of CAID material viscosity contrast (D) and buoyancy ratio (B).

- 2D spherical annulus models (figure D) exhibit fewer downwellings and reduced surface mobility as yield stress is increased.
- Using the CAID material properties shown above, the 2D model with non-dimensional yield stress 93×10^7 exhibits episodic behaviour, with a surface that transitions back and forth from mobile to stagnant over time.
- The 3D spherical model with intermediate yield stress and watershed threshold (figure C) exhibits plates that conform to a rigid velocity distribution. The correlation coefficient for the majority of detected plates exceeds 0.9. This model generates a comparable number of large plates to the present day Earth.

C.W.F. would like to acknowledge J.M Guerrero, T.T Ojo, and P. Javaheri for their work on a manuscript associated with this research. C.W.F. is grateful for funding from the Centre for Research in Earth Systems Science.

Digital Research Alliance of Canada